THE JOURNAL OF BIOLOGICAL CHEMISTRY VOL. 285, NO. 34, pp. 26088–26096, August 20, 2010

Extracellular Allosteric Regulatory Subdomain within the γ Subunit of the Epithelial Na^+ Channel*

Received for publication, May 31, 2010, and in revised form, June 25, 2010 Published, JBC Papers in Press, June 29, 2010, DOI 10.1074/jbc.M110.149963

Katie L. Winarski‡, Nan Sheng‡, Jingxin Chen‡, Thomas R. Kleyman‡§1, and Shaohu Sheng‡

From the ‡Renal-Electrolyte Division, Department of Medicine, and the §Department of Cell Biology and Physiology, School of Medicine, University of Pittsburgh, Pittsburgh, Pennsylvania 15261

The activity of the epithelial Na^+ channel (ENaC) is modulated by Na^+ self-inhibition, a down-regulation of the open probability of ENaC by extracellular Na^+. A His residue within the extracellular domain of γENaC (γHis^{239}) was found to have a critical role in Na^+ self-inhibition. We investigated the functional roles of residues in the vicinity of this His by mutagenesis and analyses of Na^+ self-inhibition responses in *Xenopus* oocytes. Significant changes in the speed and magnitude of Na^+ self-inhibition were observed in 16 of the 47 mutants analyzed. These 16 mutants were distributed within a 22-residue tract. We further characterized this scanned region by examining the accessibility of introduced Cys residues to the sulfhydryl reagent MTSET. External MTSET irreversibly increased or decreased currents in 13 of 47 mutants. The distribution patterns of the residues where substitutions significantly altered Na^+ self-inhibition or/and conferred sensitivity to MTSET were consistent with the existence of two helices within this region. In addition, single channel recordings of the γH239F mutant showed that, in the absence of Na^+ self-inhibition and with an increased open probability, ENaCs still undergo transitions between open and closed states. We conclude that γHis^{239} functions within an extracellular allosteric regulatory subdomain of the γ subunit that has an important role in conferring the response of the channel to external Na^+.

Sodium transport across apical membranes by epithelial sodium channels (ENaCs)[2] plays a critical role in regulating the extracellular fluid volume, as well as airway surface liquid volume (1). Several disorders, including Liddle syndrome and pseudohypoaldosteronism type I, result from ENaC mutations in humans (2). ENaC is regulated by many factors, which affect either channel density at the membrane surface or open probability (P_o). Among regulators of ENaC P_o is Na^+ self-inhibition, a down-regulation of both native and cloned ENaCs by extracellular Na^+. As urinary [Na^+] in distal renal tubules vary considerably under different physiological and pathological conditions, the existence of Na^+ self-inhibition provides a mechanism for epithelial cells to rapidly tune the rate of Na^+ influx according to fluctuations of the urinary [Na^+]. It may protect cells from damage by a sudden rise of intracellular [Na^+] and limit Na^+ absorption in kidney tubules to maintain body fluid balance. When the urinary [Na^+] is lower in the distal tubules, ENaCs are relieved from Na^+ self-inhibition, thus enhancing Na^+ reabsorption to minimize urinary Na^+ losses. Recent studies of the Na^+ self-inhibition response of cloned ENaCs in *Xenopus* oocytes have yielded some clues regarding this intrinsic regulatory mechanism. However, a detailed understanding of this process remains elusive.

A functional ENaC complex likely is formed by three homologous subunits in a manner similar to the trimeric structure of chicken acid-sensing ion channel 1 (cASIC1) (3), a member of the ENaC/degenerin superfamily. All three subunits contribute to the channel pore. ENaC subunits have two transmembrane domains (M1 and M2) linked by a large extracellular domain (ECD) and intracellular termini. Recent mutagenesis studies have revealed several structural elements that are required for conferring the Na^+ self-inhibition response. In a chimeric study, the proximal part of the ECD was found to control the speed of the inhibition (4). We reported that substitution of His^{239} of mouse γENaC with Asp, Arg, or Cys eliminated and the homologous mutations of αHis^{282} enhanced Na^+ self-inhibition of mouse αβγENaCs (5). All three ENaC subunits contain 16 conserved Cys residues in the ECD. Point mutations of eight α- and nine γCys residues significantly alter the Na^+ self-inhibition response, suggesting they are necessary for the formation of correct tertiary structure permitting this allosteric regulation (6). The Na^+ self-inhibition response is dramatically changed by mutations at the homologous αGly^{481} and γMet^{438} within the thumb domains of the ECD (7). In addition, several ENaC regulators, including transition metals, proteases, and extracellular H^+ and Cl^-, affect ENaC activity in part via alterations of Na^+ self-inhibition (8–14).

It appears that one of the functions of the ECDs of ENaC subunits is to confer the negative regulation by extracellular Na^+, as the mutated residues and potential sites of action for the above mentioned regulators are all within the ECDs. The crystal structure of cASIC1 revealed a highly organized ECD structure consisting of five distinct subdomains termed palm, β-ball, finger, thumb, and knuckle (3). The ECDs of ENaC subunits are expected to have a similar overall organization. However, some subdomains likely differ in structure given their limited homology. For example, sequence alignments indicate that the least conserved region between ASICs and ENaCs is in their proximal ECDs that encompasses the finger domain (3) and

* This work was supported, in whole or in part, by National Institutes of Health Grants R01 DK054354, R01 ES014701, and P30 DK079307.

[1] To whom correspondence should be addressed: Renal-Electrolyte Division, University of Pittsburgh, 3550 Terrace St., Pittsburgh, PA 15261. Tel.: 412-647-3121; Fax: 412-383-8956; E-mail: kleyman@pitt.edu.

[2] The abbreviations used are: ENaC, epithelial Na^+ channel; ASIC, acid-sensing ion channel; cASIC1, chicken ASIC1; ECD, extracellular domain; WT, wild type; MTSES, sodium (2-sulfonatoethyl)methanethiosulfonate; MTSET, [2-(trimethylammonium)ethyl]methanethiosulfonate bromide; P_o, open probability; mENaC, mouse ENaC.

contains some of the sites implicated in Na^+ self-inhibition. The poor conservation precludes the possibility of mapping these sites of interest on the cASIC1 structure with reasonable accuracy. To gain additional insights regarding the structural requirements of Na^+ self-inhibition, we systematically investigated the functional roles of selected residues in the vicinity of γHis^{239}, which we previously termed the extracellular allosteric regulatory site (EARS) (5, 8). Our data indicate that mutations of multiple residues significantly suppressed Na^+ self-inhibition and suggest that the critical γHis^{239} functions within a regulatory subdomain of 22 residues that has a specific role in conferring Na^+ self-inhibition. In addition, we demonstrate that an ENaC mutant that has lost Na^+ self-inhibition still undergoes gating transitions.

EXPERIMENTAL PROCEDURES

Site-directed Mutagenesis—Point mutations were introduced into mouse α, β, and γ ENaC ($\alpha\beta\gamma$mENaC) cDNAs in pBluescript SK-vector (Stratagene, La Jolla, CA) using the QuikChange II XL site-directed mutagenesis kit (Stratagene). The intended mutation was verified by DNA sequencing. Wild-type and mutant ENaC cRNAs were made using T3 RNA polymerase (Ambion, Inc.), purified by an RNA purification kit (Qiagen), and quantified by spectrophotometry.

ENaC Expression and Two-electrode Voltage Clamp—ENaC expression in *Xenopus* oocytes and current measurements by two-electrode voltage clamp were performed as reported previously (15). Stage V and VI oocytes with the follicle cell layer removed were injected with 50 nL/cell of mixed cRNAs composed of 0.5–2 ng of each mENaC subunit (α, β, and γ) and incubated at 18 °C in modified Barth's solution (88 mM NaCl, 1 mM KCl, 2.4 mM $NaHCO_3$, 15 mM Hepes, 0.3 mM $Ca(NO_3)_2$, 0.41 mM $CaCl_2$, 0.82 mM $MgSO_4$, 10 μg/ml streptomycin sulfate, 100 μg/ml gentamycin sulfate, pH 7.4). All experiments were performed at room temperature (20–24 °C) 20–52 h following injection. Oocytes were placed in a recording chamber from Warner Instruments (Hamden, CT) and perfused with a constant flow rate of 12–15 ml/min. Voltage clamp was performed using a TEV-200 voltage clamp amplifier (Dagan Corp.) and the DigiData 1322A interface controlled by pClamp (version 9.2, Molecular Devices Corp., Sunnyvale, CA).

Na^+ Self-inhibition—Na^+ self-inhibition was examined by rapidly replacing a low [Na^+] bath solution (NaCl-1; containing 1 mM NaCl, 109 mM *N*-methyl-D-glucamine, 2 mM KCl, 2 mM $CaCl_2$, 10 mM Hepes, pH 7.4) with a high [Na^+] bath solution (NaCl-110; containing 110 mM NaCl, 2 mM KCl, 2 mM $CaCl_2$, 10 mM Hepes, pH 7.4) while the oocytes were continuously clamped to −60 or −100 mV as specified. Bath solution exchange was done with a Teflon valve perfusion system controlled by computer (AutoMate Scientific, Inc, Berkeley, CA). Upon completion of the experiment, 10 μM amiloride was added to the bath solution to determine the amiloride-insensitive portion of the whole cell current. Inward currents present in 10 μM amiloride at −60 or −100 mV were mostly <200 nA. Data from oocytes with unusually high amiloride-insensitive currents (>5% of the total current) were eliminated to minimize current contamination from membrane leak and endogenous channels. To avoid complications from the observable variability in the Na^+ self-inhibition response of wild-type (WT) ENaCs among different batches of oocytes (6), the response of WT channels was always tested in an alternating manner with mutants in the same batch of oocytes.

An exponential equation by Clampfit (version 9.2, Molecular Devices Corp.) was used to fit the first 40 s of current decay following the maximal inward current (peak current, I_{peak}) directly after the bath solution change from a low to high Na^+ concentration. Steady state current (I_{ss}) was measured at 40 s after I_{peak}. The amiloride-insensitive currents were subtracted from I_{ss} and I_{peak} currents to determine the amiloride-sensitive current ratio of I_{ss}/I_{peak}, the index for the magnitude of Na^+ self-inhibition.

Modifying Channels with Sulfhydryl Reagents—Oocytes were perfused with NaCl-110 while clamped to −30, −60, or −100 mV. Control currents were measured for 2 min, and then the bath solution was changed to NaCl-110 supplemented with 1 mM [2-(trimethylammonium)ethyl]methanethiosulfonate bromide (MTSET, Toronto Research Chemicals, Inc.) or 5 mM sodium (2-sulfonatoethyl)methanethiosulfonate (MTSES, Toronto Research Chemicals, Inc.) for 2 min. The reagent was then washed out with NaCl-110 for 1 min, followed by perfusion with 10 μM amiloride in NaCl-110 to determine the amiloride-insensitive current. Due to the short half-life of the reagents in aqueous solutions (16), reagents were measured in powder form and dissolved in bath solution immediately prior to use. Oocytes with unstable currents were not used in these experiments.

Single Channel Recordings—Oocytes were placed in a hypertonic solution (NaCl-110 supplemented with 200 mM sucrose) for 5 min. The vitelline membranes were manually removed, and the oocytes were then placed in a recording chamber with NaCl-110 at room temperature (22–25 °C) for least 20 min before initiating recordings. The pipette solution was the same as bath solution (NaCl-110). Patch pipettes with a tip resistance of 5–10 megohms were used. Patch clamp in the cell-attached configuration was performed using a PC-One Patch Clamp amplifier (Dagan Corp.) and a DigiData 1322A interface connected to a personal computer. Patches were clamped at membrane potentials (negative value of pipette potentials) of −40 to −100 mV. pClamp (versions 8 and 10, Molecular Devices Corp.) were used for data acquisition and analyses, respectively. Single channel recordings were acquired at 5 kHz, filtered at 300 Hz by a four-pole low pass Bessel filter built in the amplifier, and stored on the hard disk. Open probability was estimated by single channel search function of pClamp (version 10) from recordings that contained no more than five current levels (four channels) and lasted for at least 5 min. Voltages were not corrected by the junction potential.

Statistical Analyses—Data are presented as mean ± S.E. Significance comparisons between groups were performed with Student's *t* tests. A p value of <0.05 was considered significantly different.

RESULTS

Aromatic Substitutions of γHis^{239} Eliminate Na^+ Self-Inhibition Response—Na^+ self-inhibition is absent in oocytes expressing $\alpha\beta\gamma$mENaC with γHis^{239} mutated to Asp, Arg, or Cys

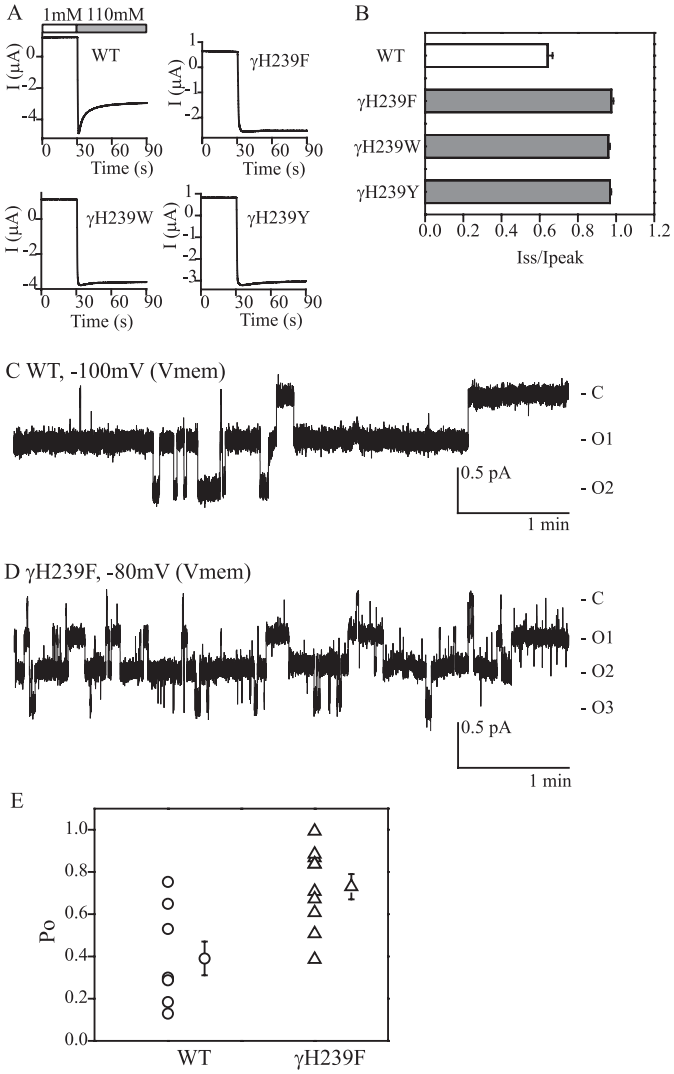

FIGURE 1. **Aromatic substitutions at γHis^{239} eliminate Na$^+$ self-inhibition.** *A*, representative recordings from oocytes expressing αβγ (*WT*), αβγH239F, αβγH239W, and αβγH239Y. Bath Na$^+$ concentrations are shown as *open* (1 mM Na$^+$) and *gray* (110 mM) *bars* in the WT recording and are omitted in the mutant recordings. *B*, ratios of I_{ss} to I_{peak}, shown as mean ± S.E. (n = 6–11). *Gray bars* indicate that values are significantly different from that of WT ($p < 0.001$). *C* and *D*, representative single channel recordings of WT and αβγH239F channels. Membrane potentials (V_{mem}) are negative values of pipette potentials. Closed and open states are identified as *C* and *O*, respectively. Current and time are shown in *scale bars*. *E*, individual P_o values of WT (*circles*) and αβγH239F (*triangles*) are shown together with the mean ± S.E. (n = 8 for WT and 10 for the mutant). The means are significantly different ($p < 0.01$).

(5). We tested whether more conservative mutations of γHis^{239} with aromatic residues would retain their functional role in the regulation of ENaC by external Na$^+$. As shown in Fig. 1, substitution of γHis^{239} with Phe, Trp, or Tyr eliminated Na$^+$ self-inhibition, suggesting this His residue has an important role in this process.

Mutations of γHis^{239} alter ENaC inhibition by extracellular Na$^+$, Ni^{2+}, and Cl$^-$, as well as ENaC activation by external Zn^{2+} and H$^+$ (5, 8, 13, 14, 17). As gating properties of γHis^{239} mutant channels have not been explored, we obtained single channel recordings of αβγH239F channels expressed in oocytes. Cell-attached patch records revealed an average P_o of αβγH239F (0.73 ± 0.06, n = 10) that was significantly higher than that of the WT (0.39 ± 0.08, n = 8, $p < 0.01$, Fig. 1). The product of P_o and channel number ($N \times P_o$) of the mutant (1.55 ± 0.23, n = 10) also was significantly greater than that of WT (0.67 ± 0.21, n = 8, $p < 0.05$). However, channel numbers in the patches were similar, 1.6 ± 0.3 (n = 10) for the mutant and 2.3 ± 0.4 (n = 8, $p > 0.05$) for WT. Single channel conductance of the mutant (4.7 ± 0.2 pS, n = 6) was not different significantly from that of WT (4.4 ± 0.1 pS, n = 7, $p > 0.05$). These results demonstrate that in the absence of a Na$^+$ self-inhibition response, ENaCs still transition between open and closed states although at a higher P_o.

Point Mutations of Residues Neighboring γHis^{239} Alter Na$^+$ Self-inhibition—To ascertain whether residues in the vicinity of γHis^{239} influence Na$^+$ self-inhibition, we performed scanning mutagenesis in the region from Ser^{214} to Glu^{261} of γmENaC. This 48-residue tract is conserved among human, mouse, and rat γENaC subunits and is predicted to contain helical, extended, and coiled structures (see Fig. 5, *A* and *B*). The 47 consecutive residues (excluding the native Cys^{220}), were mutated individually to Cys, and mutant γmENaC subunits were co-expressed with wild-type α- and βmENaCs in oocytes. Na$^+$ self-inhibition responses of the mutants were examined and compared with WT in the same batches of oocytes. Among the 47 mutants, 16 significantly altered both the speed and magnitude of Na$^+$ self-inhibition, and four increased only the time constant ($p < 0.01$, Figs. 2 and 3). A suppressed and slowed response was observed in 13 mutants (F225C, S227C, G228C, N230C, I232C, W235C, Y236C, H239C, N242C, I243C, M244C, A245C, and Q246C), and a greater and faster response was seen in the other three mutants (E234C, L238C, and Y240C). These 16 mutants, including H239C, are located in a 22-residue tract between γPhe^{225} and γGln^{246} (Fig. 3), suggesting a specific role of this segment in Na$^+$ self-inhibition. Interestingly, Fig. 3, *A* and *B*, show certain patterns in the distribution of residues where mutations led to significant changes in Na$^+$ self-inhibition. For example, from Gln^{233} to Met^{241}, three contiguous residues where substitutions altered Na$^+$ self-inhibition (Fig. 3, *black bars*) were flanked by residues where mutations did not alter Na$^+$ self-inhibition (*open bars*), suggestive of a helical structure.

Multiple Residues near γHis^{239} Are Solvent Accessible—The above distribution patterns prompted us to further probe the secondary structure(s) in the scanned region by examining accessibility of introduced Cys residues to a sulfhydryl reagent. These experiments also may provide clues regarding relative locations of the residues in the channel complex (*i.e.* exposed or buried). Positively charged and membrane impermeant MTSET was used to avoid unwanted modifications of sulfhydryl groups in transmembrane or intracellular domains of ENaCs (18, 19). Of the 47 mutants tested, external MTSET (1 mM) irreversibly inhibited four (S226C, S227C, N230C, and M241C) and activated eight (I229C, E234C, Q246C, V247C, K252C, I253C, S256C, and A259C) mutants (Figs. 3 and 4). These results indicated that at least 12 residues in the scanned region were exposed to solvent. The first seven residues modified by MTSET are within the 22-residue tract (γPhe^{225} to γGln^{246}), which hosts residues whose mutations resulted in significant changes in Na$^+$ self-inhibition. This confirms the

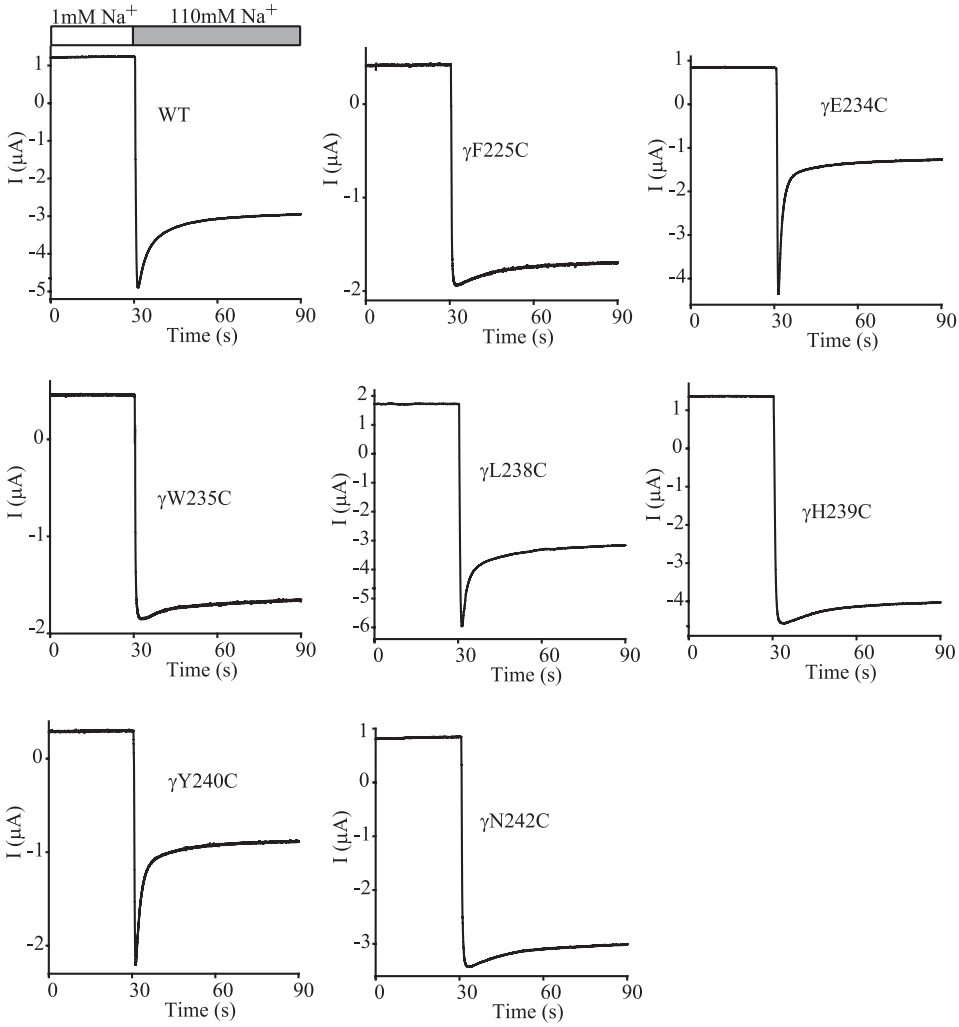

FIGURE 2. **Multiple mutations alter the Na^+ self-inhibition response.** Representative recordings for Na^+ self-inhibition responses of WT and selected mutants are shown. Oocytes were clamped at −60 mV and whole cell currents were continuously recorded, while bath [Na^+] was rapidly increased from 1 mM (*open bar*) to 110 mM (*gray bar*). The *traces* are representative of at least 13 independent observations.

important functional role of this tract. The last five sites modified by MTSET are located in a stretch of 15 residues (γVal^{247} to γGlu^{261}) immediately following the 22-residue tract. Mutations within this 15-residue tract did not significantly alter Na^+ self-inhibition, suggesting these residues are not essential to the mechanism of Na^+ self-inhibition. The observation that MTSET significantly increased currents of multiple mutants implies that this 15-residue tract also contains functionally important sites.

A lack of response to MTSET may reflect a solvent inaccessible residue. Alternatively, the residue may be accessible and modified by MTEST but lack a change in functional activity following MTSET treatment. For example, channels that lack a Na^+ self-inhibition response and have a high baseline P_o are unable respond to MTSET treatment with an increase in current. We examined whether the lack of response of γH239C to MTSET reflected a high P_o state by co-expressing γH239C with an α subunit mutant that lowers P_o (αG481M) (7). αG481M/βγH239C channels exhibited a Na^+ self-inhibition response that was significantly greater than WT (I_{ss}/I_{peak} = 0.33 ± 0.01, n = 5, $p < 0.001$ *versus* WT or αβγH239C). However, these channels did not respond to MTSET with a significant change in current (I_{MTSET}/I = 1.32 ± 0.05, n = 5, $p > 0.05$ *versus* WT), suggesting that γHis^{239} is solvent inaccessible.

The two sets of data, mutation-induced changes in Na^+ self-inhibition and responses to MTSET, allowed us to analyze potential secondary structures. Our data were consistent with an α helix comprised of residues γAla^{231}–Ile^{243}. As shown in Fig. 5*C*, all residues where mutations led to significant reductions in Na^+ self-inhibition were located on the same face in a helical wheel projection, whereas residues whose replacements did not alter or moderately enhanced Na^+ self-inhibition lined the opposite face. The two residues where introduced sulfhydryl groups were modified by MTSET shared the same face with the residues whose mutations did not suppress Na^+ self-inhibition. We attempted to map functional data to helical wheels that had various lengths and starting residues. The above 13-residue helix was the one most compatible with all three criteria: secondary structural predictions (Fig. 5*B*), mutation-induced changes in Na^+ self-inhibition, and responses to MTSET (Fig. 3). In addition, the four residues whose substitutions by Cys residues rendered the mutants responding to MTSET with irreversible increases in currents line the same face of a helical wheel comprising 10 residues from γGlu^{250} to γAla^{259}, suggesting a second helical structure (Fig. 5*D*). For residues between γPhe^{225} and γAsn^{230}, no consensus secondary structures could be elucidated from our functional studies.

Functional role of γGlu^{234}—Of all of the mutants tested, MTSET had the greatest effect on γE234C with an I_{MTSET}/I of 3.2 ± 0.2 (n = 27). The large stimulatory effect was somewhat surprising given the moderate enhancement of Na^+ self-inhibition observed with this mutation (Figs. 2 and 3). We performed additional studies to examine the functional role of γGlu^{234}. Substitutions with Gln, Lys, or Arg showed an enhancement of Na^+ self-inhibition similar to that of γE234C. The I_{ss}/I_{peak} values were 0.47 ± 0.02 (n = 6) for γE234Q, 0.41 ± 0.02 (n = 6) for γE234K, 0.44 ± 0.02 (n = 6) for γE234R, and 0.59 ± 0.02 (n = 6) for WT. The time constants were 5.2 ± 0.3 (n = 6) for γE234Q, 5.0 ± 0.3 (n = 6) for γE234K, 5.1 ± 0.3 (n = 6) for γE234R, and 7.8 ± 0.2 (n = 6) for WT. All above values for the mutants significantly were less than that of WT ($p < 0.01$). The results suggest that γGlu^{234} is not critical for the Na^+ self-

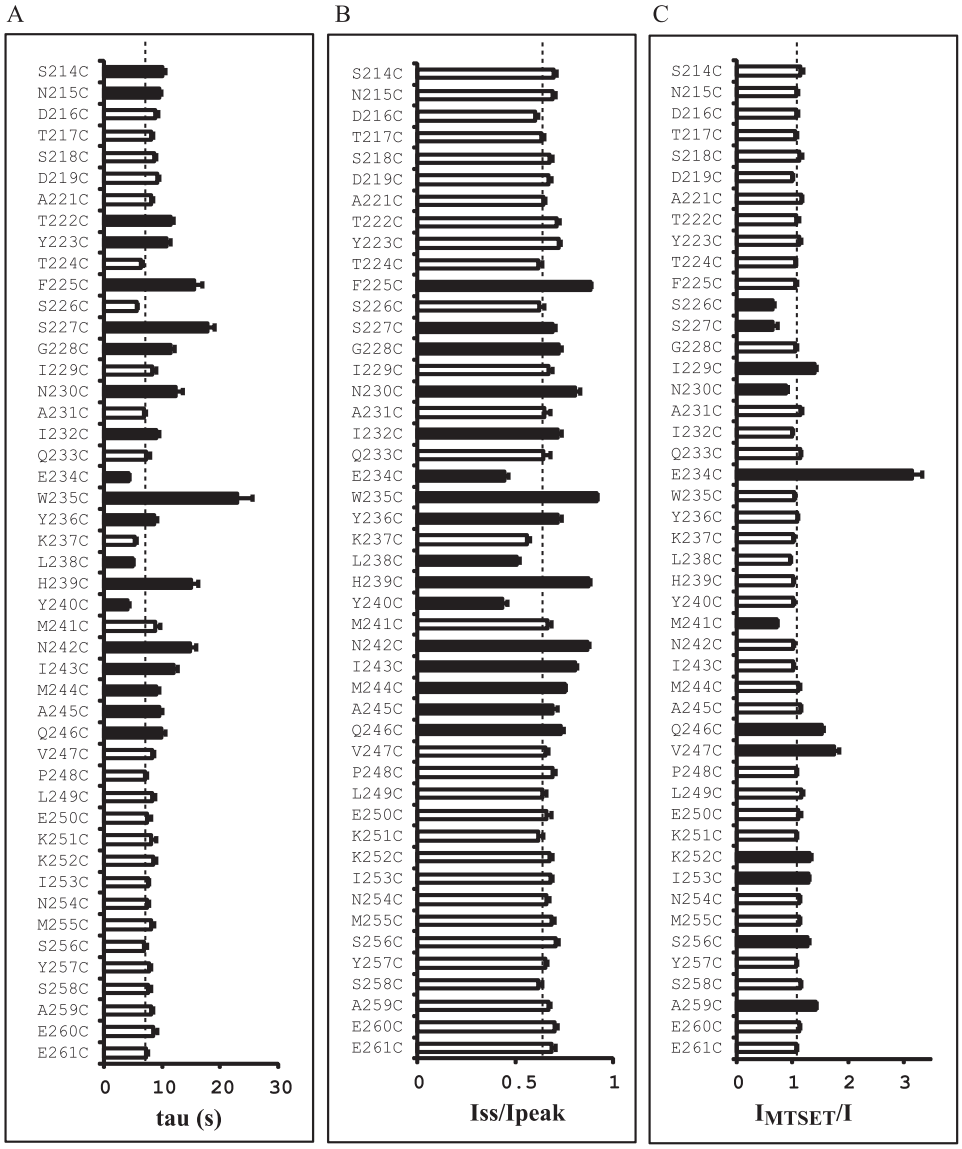

FIGURE 3. **Effects of mutations on Na^+ self-inhibition and MTSET responses.** *A*, time constants (tau) for current decays representing Na^+ self-inhibition. *B*, I_{ss}/I_{peak}. Values in *A* and *B* were obtained as described under "Experimental Procedures." Data were collected in different batches of oocytes. Student's *t* tests were performed in the same batch of oocytes to compare the Na^+ self-inhibition responses of WT and an individual mutant. Values that are significantly different from that of WT are shown as *black bars* ($p < 0.01$). *Dashed lines* show the averaged WT values representing 133 observations from 21 batches of oocytes, which are intended for reference and not for statistical comparisons. The values of the mutants were obtained from 6–30 oocytes. *C*, ratios of the current after a 2-min MTSET treatment (I_{MTSET}) and current prior to the treatment (I, $n = 4$–27). The I_{MTSET}/I values were calculated from amiloride-sensitive currents. Student's *t* tests were performed in the same batches of oocytes to compare the I_{MTSET}/I values of WT and an individual mutant. For some mutants, results from several batches of oocytes were pooled in the same manner as for WT. Values that are significantly different from that of WT ($p < 0.01$) are shown as *black bars*. The I_{MTSET}/I values of all the mutants shown in *black bars* are significant from WT ($p < 0.01$, paired Student's *t* test). The *dashed line* shows the averaged I_{MTSET}/I of WT obtained by pooling all data from 48 oocytes.

these data suggest that access to γE234C is not charge-dependent but the modification-induced effect requires a positive charge.

We tested whether the large activation of αβγE234C channels by MTSET resulted from a suppression of Na^+ self-inhibition by comparing self-inhibition responses before and after MTSET modification. As shown in Fig. 6*D*, Na^+ self-inhibition was reduced greatly but not eliminated. A similar result was observed in oocytes treated with MTSET in the low Na^+ bath solution (Fig. 6*E*), indicating that the introduced Cys was accessible in both a low and high [Na^+] bath. These observations suggest that MTSET activated γE234C by primarily suppressing Na^+ self-inhibition and thus increasing channel P_o, and that MTSET modification under the current experimental conditions was insufficient to eliminate Na^+ self-inhibition.

If MTSET activates γE234C channels by suppressing Na^+ self-inhibition, the expression of γE234C with an additional mutation that eliminates Na^+ self-inhibition should blunt the activation by MTSET. We expressed γE234C with additional mutations including γH239R, γR143A-Δ144–186, and βS518K. Mutant mENaCs with γH239R had no Na^+ self-inhibition response (5). The degeneration mutation βS518K has a P_o of ~1 (20, 21) and is expected to have no Na^+ self-inhibition response. Indeed, we observed no Na^+ self-inhibition in oocytes expressing αβS519Kγ mENaC ($I_{ss}/I_{peak} = 0.95 \pm 0.02$, $n = 4$, $p < 0.001$ *versus* WT). γR143A-Δ144–186 channels also have a high P_o (>0.95) (22). Na^+ self-inhibition was not observed in oocytes expressing this mutant ($I_{ss}/I_{peak} = 0.99 \pm 0.01$, $n = 6$, $p < 0.001$ *versus* WT). As expected, these double mutant channels (γE234C with γH239R, βS518K, or γR143A-Δ144–186) showed little or no Na^+ self-inhibition response, and their response to MTSET was dramatically blunted (Fig. 7 and Table 1).

inhibition response and rather may function as a moderate suppressor of Na^+ self-inhibition in WT channels.

To test whether modification of γE234C is charge-dependent, we examined the effect of a negatively charged sulfhydryl reagent, MTSES. As shown in Fig. 6*B*, 5 mM MTSES did not significantly alter whole cell Na^+ currents. However, MTSES application blocked the stimulatory effect of MTSET (Fig. 6*C*), indicating that the mutant was modified by MTSES without an observable change in current. As MTSET and MTSES have similar volumes but carry opposite charges at neutral pH (16),

DISCUSSION

We demonstrated previously that γHis^{239} has an important role in Na^+ self-inhibition, based on the absence of an inhibi-

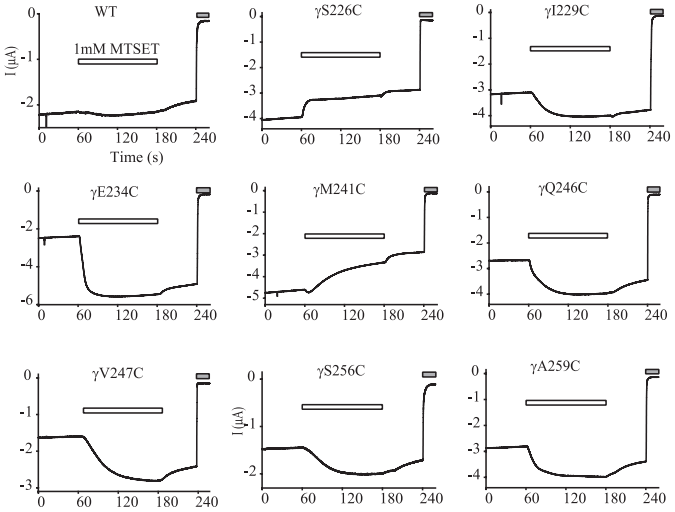

FIGURE 4. **MTSET modification of introduced Cys residues.** Oocytes were clamped at −60 mV, and whole cell currents were continuously recorded prior to, during (*open bars*) and after bath application of 1 mM MTSET. The *gray bars* indicate the presence of 10 μM amiloride. The traces are representative of at least five independent observations.

tory response in mutant channels with γH239D, γH239R, or γH239C mutations (5). In the current study, we found that more conservative substitutions of γHis^{239} with amino acids bearing aromatic side chains (Phe, Tyr, or Trp) also eliminated Na^+ self-inhibition. These results suggest that the side chain of γHis^{239} is required for channels to respond to external Na^+ with a reduction in channel P_o.

Single channel recordings indicated that the γH239F mutation, which eliminated Na^+ self-inhibition, increased the average P_o compared with WT but retained otherwise typical transitions between closed and open states. This observation is consistent with previously published work demonstrating that the magnitude of Na^+ self-inhibition is an important factor determining channel P_o in the presence of extracellular Na^+ (7, 11). The previously described populations of ENaCs with a high P_o (≥0.75) (23) likely correspond to channels with blunted or absent Na^+ self-inhibition. Our observation that ENaCs lacking Na^+ self-inhibition still undergo typical transitions between closed and open states suggests that channel gating is not controlled solely by Na^+ self-inhibition. External Na^+ is one of the factors that govern the intrinsic gating of ENaC.

We found that multiple mutations in the neighborhood of γHis^{239} dramatically altered Na^+ self-inhibition. In fact, four mutants (γF225C, γN230C, γW235C, and γN242C) in addition to γH239C nearly eliminated Na^+ self-inhibition. These results suggest that a subdomain, comprising a stretch of 22 residues from γPhe^{225} to γGln^{246} that encompasses all residues where mutations led to significant changes in both the speed and magnitude of Na^+ self-inhibition (Fig. 3), has a significant role in the mechanism of Na^+ self-inhibition. The 25 residues flanking this 22-residue tract do not appear to have an important role in Na^+ self-inhibition, as Cys mutations produced either no change in the magnitude of Na^+ self-inhibition (I_{ss}/I_{peak}) or only moderate changes in the time constants (Fig. 3). This 22-residue tract is likely within the finger domain of the γ subunit, a region that is predicted to be in the periphery of the ECD where many residues are likely to be solvent accessible (3, 24).

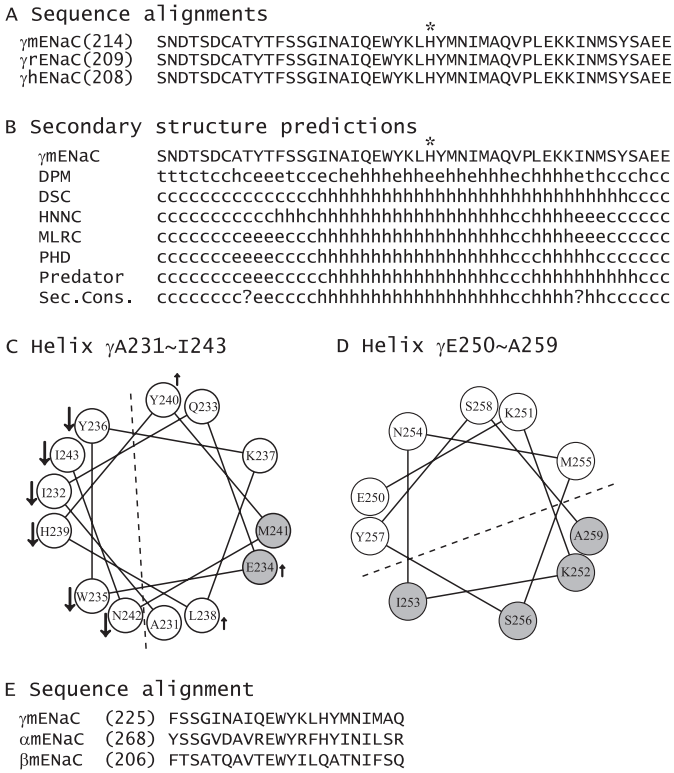

FIGURE 5. **Secondary structure predictions.** *A*, sequence alignments of the segments corresponding to γSer^{214}–Glu^{261} of mENaC. The alignments of γ subunits of mouse, rat, and human ENaCs were performed with Vector NTI 11.0 (Invitrogen), and only the regions of interest are shown. The full-length identities at the amino acid level are 97% between γmENaC and γrENaC and 86% between γmENaC or γrENaC and γhENaC. γHis^{239} is identified by an *asterisk*. *B*, secondary structure predictions of the mutated region of γmENaC. The predictions were performed with Network Protein Sequence Analysis (38). *h*, helical; *e*, extended; *t*, turn; and *c*, coiled. *C* and *D*, helical wheel projections. The helical wheels were generated with Membrane Protein Explorer (version 3.1) (39). Residues where mutations resulted in significant reductions or enhancements of Na^+ self-inhibition, compared with WT, are identified by *downward arrows* and *upward arrows*, respectively. *Gray spheres* denote the residues where Cys substitutions led to significant changes in currents following MTSET application. A *dashed line* separates the two faces with distinct changes on the projected helical wheel. *E*, sequence alignments of the segments corresponding to the 22-residues tracts within γmENaC (γPhe^{225}–γGln^{246}), αmENaC, and βmENaC.

The modification of introduced Cys residues at multiple sites by MTSET confirms that some residues in the scanned region are solvent accessible. The 22-residue tract in the γ subunit is conserved moderately, as 15 of 22 residues are identical or conserved among the three subunits (Fig. 5*E*). Mutations at selected sites in the related 22-residue tract in the α subunit enhanced Na^+ self-inhibition.[3] However, this tract is not present within ASICs. We suggest that this tract constitutes a regulatory module to confer Na^+ self-inhibition (*i.e.* an Na^+ self-inhibition module). Upstream of this region are the previously identified cleavage sites for furin, prostasin, neutrophil elastase, plasmin, and channel-activating proteas 2 (22, 25–28). Proteases activate ENaC by releasing inhibitory tracts that, when present, enhance Na^+ self-inhibition (10–12, 29). Our current observations and previous studies (5, 7, 22, 27, 29–35) support the notion that the γ subunit plays an important role in control-

[3] O. B. Kashlan, C. R. Boyd, C. Argyropoulos, S. Okumora, R. P. Hughey, M. Grabe, and T. R. Kleyman, unpublished observations.

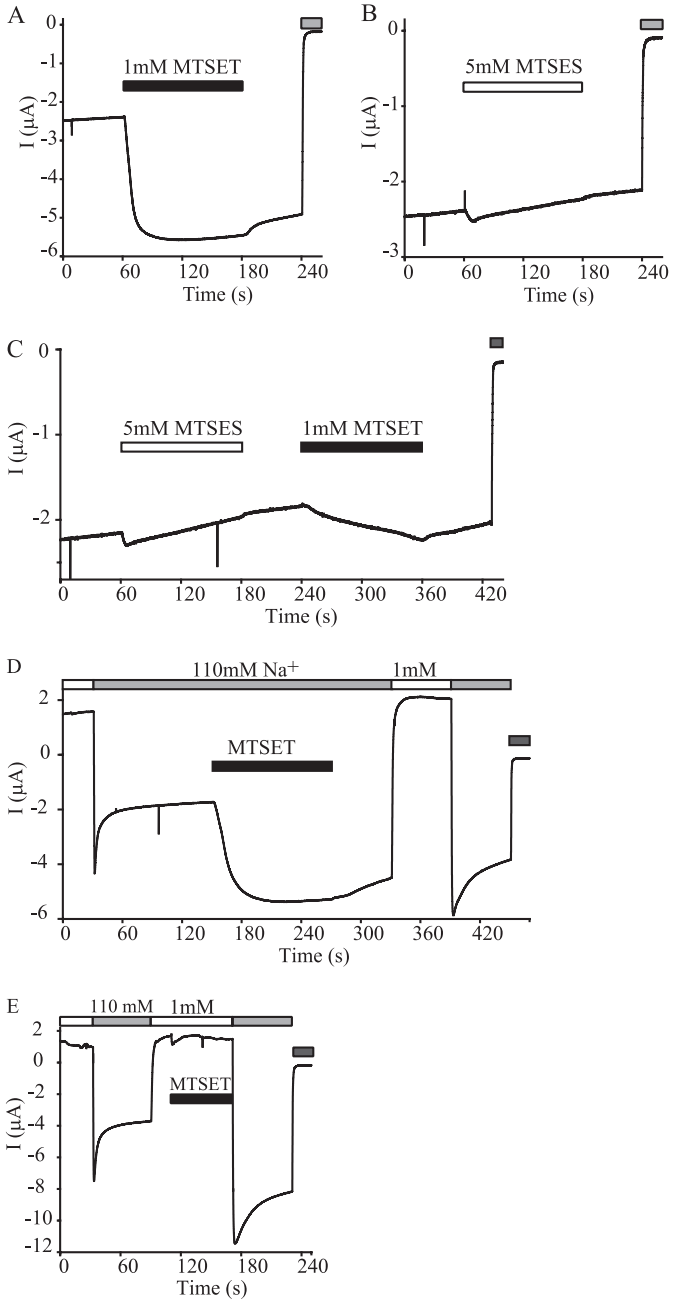

FIGURE 6. **Effects of MTSET and MTSES on $\alpha\beta\gamma$E234C.** Experiments were similar to those in Fig. 4. Recordings representative of at least five oocytes expressing $\alpha\beta\gamma$E234C are shown. The *gray bars* at the end of recording traces indicate the presence of 10 μM amiloride. *A*, typical response of $\alpha\beta\gamma$E234C to 1 mM MTSET. *B*, representative recording of $\alpha\beta\gamma$E234C current prior to, during (*open bar*), and after application of 5 mM MTSES. *C*, a recording showing the responses to 5 mM MTSES (*open bar*) and subsequent 1 mM MTSET (*black bar*). *D*, Na^+ self-inhibition responses before and after 1 mM MTSET treatment. MTSET was applied in 110 mM Na^+ bath solution (*black bar*). *E*, Na^+ self-inhibition responses before and after 1 mM MTSET treatment. MTSET was applied in 1 mM Na^+ bath solution (*black bar*).

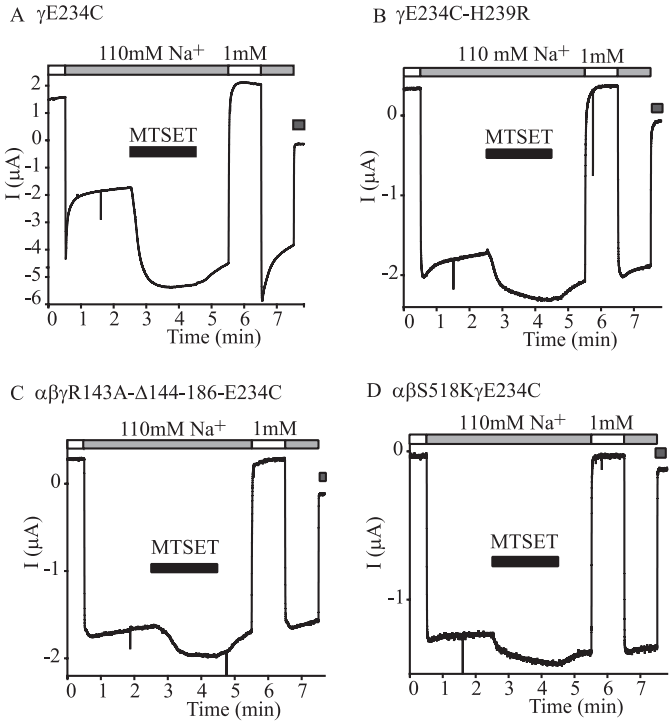

FIGURE 7. **Activation of $\alpha\beta\gamma$E234C by MTSET depends on the presence of an Na^+ self-inhibition response.** The same method as described in Fig. 6*D* was used to examine the effects of 1 mM MTSET on the currents and Na^+ self-inhibition responses in oocytes expressing $\alpha\beta\gamma$E234C (*A*), $\alpha\beta\gamma$E234C-H239R (*B*), $\alpha\beta\gamma$R143A-Δ144–186-E234C (*C*), or $\alpha\beta$S518K/γE234C (*D*). Application of MTSET is shown (*black bar*). The *gray bars at the end of the traces* indicate the presence of 10 μM amiloride. The responses of each group were examined in at least four oocytes.

TABLE 1

Effects of MTSET on currents and magnitudes of Na^+ self-inhibition in mutants containing γE234C alone or in combination with an additional mutation

I_{MTSET}/I was the ratio of the amiloride-sensitive current following 1 mM MTSET treatment for 2 min and the current before the treatment. $I_{ss}/I_{peak}{}^1$ and $I_{ss}/I_{peak}{}^2$ were obtained prior to and after MTSET treatment in the same oocyte, respectively. Values are mean ± S.E.

Channel	Oocytes	$I_{ss}/I_{peak}{}^1$	I_{MTSET}/I	$I_{ss}/I_{peak}{}^2$
$\alpha\beta\gamma$E234C	5	0.40 ± 0.01	3.43 ± 0.07	0.72 ± 0.01
$\alpha\beta\gamma$E234C-H239R	4	0.89 ± 0.01[a]	1.32 ± 0.02[a]	0.93 ± 0.00[a]
$\alpha\beta\gamma$E234C/R143A-Δ144–186	5	0.98 ± 0.02[a]	1.23 ± 0.01[a]	0.96 ± 0.01[a]
$\alpha\beta$S518KγE234C	5	0.96 ± 0.01[a]	1.19 ± 0.03[a]	0.96 ± 0.01[a]

[a] $p < 0.01$ *versus* $\alpha\beta\gamma$E234C.

ling the gating of the trimeric ENaC and mediating channel regulation by various factors.

We used three independent measures to probe the secondary structure of the scanned region: sequence-based secondary structural predictions, analyses of the periodicity of mutation-induced changes in Na^+ self-inhibition, and analyses of the periodicity of solvent accessibility. We identified two potential α helices, comprising residues γAla^{231}–γIle^{243} and residues γGlu^{250}–γAla^{259} (Fig. 5*C*). The helical wheel projection in Fig. 5*C* shows that all residues whose substitutions by Cys significantly suppressed Na^+ self-inhibition line one face, suggesting that a functional role is confined to one face of the helix. Interestingly, three adjacent residues (Trp^{235}, His^{239}, and Asn^{242}) showed the greatest reductions in Na^+ self-inhibition with Cys substitutions. As channels with Cys mutations at these sites did not respond to MTSET, they may be solvent inaccessible to MTSET. However, we cannot rule out the possibility that some Cys residues were modified by MTSET without detectable change in currents. Within the residues γAla^{231}–γIle^{243} comprising a putative helix, only two Cys substitution (γE234C and γM241C) were clearly modified by MTSET and were on a face of the helix that was clearly distinct from the face where Cys

substitutions affected Na^+ self-inhibition (Fig. 5*C*). These results suggest that the face of the helix with residues that have a functional role in Na^+ self-inhibition interact with other components of the channel complex, shielding these residues from the solvent. We also identified a second helix (γGlu^{250}–γAla^{259}, Fig. 5*D*), based on the accessibility of Cys mutants to MTSET. This distal helix did not appear to have a role in conferring changes in P_o in response to external Na^+, as Cys mutants in this distal helix did not affect the Na^+ self-inhibition response.

Sequence alignments and previous publications (3, 29, 36) suggest that a subdomain corresponding to the finger in the cASIC1 structure contains both previously identified protease cleavage sites and the region scanned in this study. The finger domain in the cASIC1 structure is formed by three helices, α1 (11 residues), α2 (10 residues), and α3 (15 residues with a disruption in the helix), together with connecting loops. Due to low homology at the finger region between cASIC1 and γmENaC (11% identity and 34% similarity) and the presence of 88 extra residues in γmENaC compared with cASIC1 (152 *versus* 64 residues between α1 and α3), it is difficult to build a homology model for γmENaC using the cASIC1 structure. Furthermore, it is not clear whether our proposed helices correspond to helices in the finger domain of the cASIC1 structure.

We identified previously a 43-residue inhibitory tract within the finger domain of the γ subunit that is released by proteolytic processing by furin and prostasin (22, 29). At present, it is unclear whether there are direct interactions between this inhibitory tract and the 22-residue tract we have identified. The loss of Na^+ self-inhibition when the 43-residue inhibitory tract is deleted (Fig. 7*C*) or with mutations of key residues within the 22-residue tract (Figs. 1–3 and 5) suggest that these regions might interact. Based on observations that mutations in the finger and thumb domains affect Na^+ self-inhibition (5–7, 11, 14), we suggest that the regulation of channel gating by external Na^+ involves transitions in both the finger and thumb domains that are eventually transmitted to the gate of the channel.

γGlu^{234} does not appear to be critical for the Na^+ self-inhibition response, given the observed moderate increase in the speed and magnitude of the current decay with four distinct substitutions (Cys, Gln, Lys, or Arg). In contrast, modification of γE234C by MTSET led to a dramatic increase in current that was largely attributable to suppression of Na^+ self-inhibition (Figs. 4, 6, and 7). Negatively charged MTSES, which is similar in size to MTSET, was able to modify the γE234C mutant (*i.e.* block the effect of MTSET) but did not activate the channel (Fig. 6). The different effects of γGlu^{234} substitutions by positively charged Lys and Arg *versus* MTSET modification suggest that size of the side chain at this position, in addition to charge, influences Na^+ self-inhibition. The MTSET-modified side chain of Cys (173 $Å^3$) is considerably larger than that of Lys (97 $Å^3$) or Arg (115 $Å^3$) (37).

In summary, we observed that Cys substitutions at multiple sites within the vicinity of the γHis^{239} dramatically suppressed the Na^+ self-inhibition response. These residues are clustered within a stretch of 22 residues from Phe^{225} to Gln^{246}. Within this 22-residue tract is a putative α helix (residues γAla^{231}–Ile^{243}). We propose that this 22-residue tract functions as an extracellular allosteric regulatory subdomain to specifically modulate Na^+ self-inhibition. Whether this subdomain contributes to a Na^+ binding pocket or participates in conformational changes that relay the local effect of Na^+ binding to the channel gate remains to be determined.

Acknowledgment—We thank Ted Schroeder for generating three His^{239} mutations.

REFERENCES

1. Sheng, S., Johnson, J. P., and Kleyman, T. R. (2007) in *Seldin and Giebisch's The Kidney: Physiology & Pathophysiology* (Alpern, R. J., and Hebert, S. C. eds) 4th Ed., pp. 743–768, Academic Press, New York
2. Rossier, B. C., Pradervand, S., Schild, L., and Hummler, E. (2002) *Annu. Rev. Physiol.* **64,** 877–897
3. Jasti, J., Furukawa, H., Gonzales, E. B., and Gouaux, E. (2007) *Nature* **449,** 316–323
4. Babini, E., Geisler, H. S., Siba, M., and Gründer, S. (2003) *J. Biol. Chem.* **278,** 28418–28426
5. Sheng, S., Bruns, J. B., and Kleyman, T. R. (2004) *J. Biol. Chem.* **279,** 9743–9749
6. Sheng, S., Maarouf, A. B., Bruns, J. B., Hughey, R. P., and Kleyman, T. R. (2007) *J. Biol. Chem.* **282,** 20180–20190
7. Maarouf, A. B., Sheng, N., Chen, J., Winarski, K. L., Okumura, S., Carattino, M. D., Boyd, C. R., Kleyman, T. R., and Sheng, S. (2009) *J. Biol. Chem.* **284,** 7756–7765
8. Sheng, S., Perry, C. J., and Kleyman, T. R. (2004) *J. Biol. Chem.* **279,** 31687–31696
9. Yu, L., Eaton, D. C., and Helms, M. N. (2007) *Am. J. Physiol. Renal Physiol.* **293,** F236–244
10. Chraïbi, A., and Horisberger, J. D. (2002) *J. Gen. Physiol.* **120,** 133–145
11. Sheng, S., Carattino, M. D., Bruns, J. B., Hughey, R. P., and Kleyman, T. R. (2006) *Am. J. Physiol. Renal Physiol.* **290,** F1488–1496
12. Bize, V., and Horisberger, J. D. (2007) *Am. J. Physiol. Renal Physiol.* **293,** F1137–1146
13. Collier, D. M., and Snyder, P. M. (2009) *J. Biol. Chem.* **284,** 792–798
14. Collier, D. M., and Snyder, P. M. (2009) *J. Biol. Chem.* **284,** 29320–29325
15. Sheng, S., Li, J., McNulty, K. A., Avery, D., and Kleyman, T. R. (2000) *J. Biol. Chem.* **275,** 8572–8581
16. Karlin, A., and Akabas, M. H. (1998) *Methods Enzymol.* **293,** 123–145
17. Sheng, S., Perry, C. J., and Kleyman, T. R. (2002) *J. Biol. Chem.* **277,** 50098–50111
18. Snyder, P. M., Olson, D. R., and Bucher, D. B. (1999) *J. Biol. Chem.* **274,** 28484–28490
19. Kellenberger, S., Gautschi, I., Pfister, Y., and Schild, L. (2005) *J. Biol. Chem.* **280,** 7739–7747
20. Snyder, P. M., Bucher, D. B., and Olson, D. R. (2000) *J Gen Physiol.* **116,** 781–790
21. Condliffe, S. B., Zhang, H., and Frizzell, R. A. (2004) *J. Biol. Chem.* **279,** 10085–10092
22. Bruns, J. B., Carattino, M. D., Sheng, S., Maarouf, A. B., Weisz, O. A., Pilewski, J. M., Hughey, R. P., and Kleyman, T. R. (2007) *J. Biol. Chem.* **282,** 6153–6160
23. Palmer, L. G., and Frindt, G. (1996) *J Gen. Physiol.* **107,** 35–45
24. Gonzales, E. B., Kawate, T., and Gouaux, E. (2009) *Nature* **460,** 599–604
25. Hughey, R. P., Bruns, J. B., Kinlough, C. L., Harkleroad, K. L., Tong, Q., Carattino, M. D., Johnson, J. P., Stockand, J. D., and Kleyman, T. R. (2004) *J. Biol. Chem.* **279,** 18111–18114
26. Adebamiro, A., Cheng, Y., Rao, U. S., Danahay, H., and Bridges, R. J. (2007) *J Gen Physiol.* **130,** 611–629
27. Passero, C. J., Mueller, G. M., Rondon-Berrios, H., Tofovic, S. P., Hughey, R. P., and Kleyman, T. R. (2008) *J. Biol. Chem.* **283,** 36586–36591
28. García-Caballero, A., Dang, Y., He, H., and Stutts, M. J. (2008) *J Gen. Physiol.* **132,** 521–535
29. Kleyman, T. R., Carattino, M. D., and Hughey, R. P. (2009) *J. Biol. Chem.* **284,** 20447–20451

30. Fyfe, G. K., and Canessa, C. M. (1998) *J Gen. Physiol.* **112,** 423–432
31. Ji, H. L., and Benos, D. J. (2004) *J. Biol. Chem.* **279,** 26939–26947
32. Carattino, M. D., Sheng, S., and Kleyman, T. R. (2005) *J. Biol. Chem.* **280,** 4393–4401
33. Carattino, M. D., Hughey, R. P., and Kleyman, T. R. (2008) *J. Biol. Chem.* **283,** 25290–25295
34. Diakov, A., Bera, K., Mokrushina, M., Krueger, B., and Korbmacher, C. (2008) *J Physiol.* **586,** 4587–4608
35. Frindt, G., and Palmer, L. G. (2009) *Am. J. Physiol. Renal Physiol.* **297,** F1249–1255
36. Stockand, J. D., Staruschenko, A., Pochynyuk, O., Booth, R. E., and Silverthorn, D. U. (2008) *IUBMB Life* **60,** 620–628
37. Ma, C., Remani, S., Sun, J., Kotaria, R., Mayor, J. A., Walters, D. E., and Kaplan, R. S. (2007) *J. Biol. Chem.* **282,** 17210–17220
38. Combet, C., Blanchet, C., Geourjon, C., and Deléage, G. (2000) *Trends Biochem. Sci.* **25,** 147–150
39. Snider, C., Jayasinghe, S., Hristova, K., and White, S. H. (2009) *Protein Sci.* **18,** 2624–2628